Stochastic Coagulation and the Timescale for Runaway Growth

Leonid Malyshkin and Jeremy Goodman

Princeton University Observatory, Princeton, NJ 08544
E-mail: leonmal@astro.princeton.edu

ABSTRACT

We study the stochastic coagulation equation using simplified models and efficient Monte Carlo simulations. It is known that (i) runaway growth occurs if the two-body coalescence kernel rises faster than linearly in the mass of the heavier particle; and (ii) for such kernels, runaway is instantaneous in the limit that the number of particles tends to infinity at fixed collision time per particle. Superlinear kernels arise in astrophysical systems where gravitational focusing is important, such as the coalescence of planetesimals to form planets or of stars to form supermassive black holes. We find that the time required for runaway decreases as a power of the logarithm of the the initial number of particles. Astrophysical implications are briefly discussed.

Key Words: planetesimals, planetary formation; collisional physics; methods, numerical.

1. Introduction

A frequently-encountered process in many fields of science is the random coalescence of small bodies into larger ones, conserving total mass. Astrophysical examples include the coalescence of planetesimals into planets (Safronov 1969) and of stars into black holes (Lee 1987; Quinlan and Shapiro 1990). When the number of bodies is large, coalescence is often modeled by Smoluchowski's equation (Smoluchowski 1916), also known as the *statistical equation*:

$$\frac{dc_i}{d\tau} = \frac{1}{2}\sum_{j=1}^{i-1} K(i-j,j)c_{i-j}c_j - c_i\sum_{j=1}^{\infty} K(i,j)c_j, \tag{1}$$

Here the *concentration* $c_i(\tau)$ is the number of bodies per unit volume of mass $m_i \propto i$ at time τ, and the functional form of the *coagulation kernel* $K(i,j) = K(j,i)$ is chosen to approximate the mass dependence of the two-body collision rate.

The statistical equation is intended to model coalescence on average, smoothing over fluctuations. It is not expected to be accurate when the initial number of particles, N, is

small. More interestingly, eq. (1) can fail even for $N \gg 1$ if $K(i,j)$ increases sufficiently rapidly with i and j. Coalescence should conserve mass, so that the mass density

$$\rho(\tau) \stackrel{\rm def}{=} \sum_{k=1}^{\infty} k\, c_k(\tau)$$

is constant. It is easy to show from eq. (1) that $\dot\rho = 0$ provided that the relevant summations converge and can be interchanged. But in the analytic solution of the case $K(i,j) = ij$ starting from the *monodisperse* initial conditions

$$c_i(0) = \delta_{i1}, \qquad \rho(0) = \frac{N}{V} = 1, \tag{2}$$

$\rho(\tau)$ begins to decrease after $\tau = 1$ (Trubnikov 1971). This is usually interpreted to mean that a macroscopic *runaway particle* has formed—also known as a *gel*, because of applications in physical chemistry. It is believed that for $K(i,j) \sim (ij)^\nu$ with $\nu > 1$, gelation begins immediately in the statistical equation (Jeon 1999; Lee 2000, and references therein). The model (1) can be extended to include the gel/runaway particle explicitly (Flory 1953). Monte Carlo simulations for large but finite N show, however, that such models do not accurately predict the time dependence of the gel mass even on average if $\nu > 1$ (Spouge 1985).

Coagulation is more correctly described by the *stochastic* equation for the joint probability $f(n_1, n_2, \ldots; t)$ for the occupation numbers $\{n_1, n_2, \ldots\}$ of the mass bins:

$$\begin{aligned}
\frac{\partial}{\partial t} f(\mathbf{n};t) &= \sum_{i=1}^{N} \sum_{j=i+1}^{N} K(i,j)\,(n_i+1)(n_j+1) f(\ldots, n_i+1, \ldots, n_j+1, \ldots, n_{i+j}-1, \ldots; t) \\
&+ \sum_{i=1}^{N} \frac{1}{2} K(i,i)\,(n_i+2)(n_i+1) f(\ldots, n_i+2, \ldots, n_{2i}-1, \ldots; t) \\
&- \sum_{i=1}^{N} \sum_{j=i+1}^{N} K(i,j)\, n_i n_j f(\mathbf{n};t) \;-\; \sum_{i=1}^{N} \frac{1}{2} K(i,i)\, n_i(n_i-1) f(\mathbf{n};t),
\end{aligned} \tag{3}$$

The statistical equation results from taking first moments,

$$c_i(t) \stackrel{\rm def}{=} V^{-1}\, \overline{n}_i(t) \stackrel{\rm def}{=} V^{-1} \int n_i f(n_1, \ldots, n_{i-1}, n_i, n_{i+1}, \ldots; t)\, dn_1 \ldots dn_{i-1} dn_{i+1} \ldots, \tag{4}$$

in the limit that $N, V \to \infty$ at fixed $\rho(0)$. In order to get a closed set of equations, one assumes that $\overline{n_i n_j} = \overline{n}_i \times \overline{n}_j$. This is justified if the occupation numbers are approximately uncorrelated. But if runaway should occur, then the occupation numbers of all the low-mass bins are correlated with bins $i \sim N$ traversed by the runaway particle.

Like the statistical equation, the stochastic equation has analytic solutions for the kernels $K(i,j) \propto$ constant, $i+j$, and $i \times j$ (Lushnikov 1977; Tanaka and Kiyoshi 1993). For the first two kernels, the predictions of the two equations are compatible in the following sense: after monodisperse initial conditions, $c_i(\tau)$ computed from eq. (1) agrees with $c_i(t)$ computed from eqs. (3)-(4) in the limit $N \to \infty$ if t and τ are related by the initial collision time per particle,

$$t_{\rm coll} \stackrel{\rm def}{=} [(N-1)\,K(1,1)]^{-1}\,, \qquad \tau = t/t_{\rm coll}. \tag{5}$$

For these kernels, there is no runaway, and the statistical equation conserves mass. Even for $K(i,j) = ij$, a similar agreement is found between the statistical and stochastic equations at $\tau < 1$ and mass bins $i \ll \sqrt{N}$ (Tanaka and Kiyoshi 1993). The stochastic equation confirms that runaway begins at $\tau > 1$; more precisely, Lushnikov (1977) shows that the quantity

$$\kappa(\tau) \stackrel{\rm def}{=} \lim_{N\to\infty} \left[N^{-2} \sum_{i=1}^{N} i^2\, \overline{n}_i(\tau) \right],$$

which can be interpreted as the runaway mass fraction on average, becomes nonzero at $\tau = 1$ and $\approx 1 - 2e^{-\tau}$ at $\tau \gg 1$.

Kernels such that $K(i,j) \propto i^\nu$ when $i \gg j$ are sometimes called "unphysical" if $\nu > 1$ because if collision rate were proportional to surface area, then surface area would have to increase more rapidly than mass. But in astrophysics (and elsewhere), gravitational focusing and mass stratification may conspire to produce $\nu > 1$ (§5). Thus a better term for such kernels would be *superlinear*. The occurrence and timescale of runaway are of great interest since the runaway particle may represent a planet or supermassive black hole, for example. Unfortunately, few general results are known for the superlinear regime. Spouge (1985) conjectured on the basis of Monte Carlo simulations of stochastic coagulation that *runaway is instantaneous for* $\nu > 1$ *in the limit* $N \to \infty$: in other words, the entire mass is consumed by a single particle after an infinitesimal multiple of the single-particle collision time $t_{\rm coll}$. A similar conjecture had previously been made by Domilovskii, Lushikov, and Piskunov (1978) for the special case $\nu = 3$, also on the basis of Monte-Carlo simulations. Recently, Jeon (1999) has supplied a proof.

Clearly, runaway/gelation is not instantaneous for finite N. To the best of our knowledge, there have been no general and quantitative statements about the scaling of the runaway time with N, although the question is an important one since N is never truly infinite in practical applications. The main result of the present paper will be the conjecture, supported by Monte Carlo simulations, that $\tau_{\rm runaway}$ varies as a negative power of $\log N$ for $\nu > 1$. Even before performing our simulations, we were lead to this conjecture on the basis of the highly simplified model presented in §2. Our Monte Carlo algorithm for stochastic

coagulation is described in §3 and tested against the analytic solutions of the stochastic equation cited above. Simulations for $\nu > 1$ are reported in §4. Finally, in §5, we discuss applications of our conjecture to cases of astrophysical importance.

2. MONOTROPHIC MODEL

The full stochastic equation seems to be analytically intractable for general values of the merging exponent ν. In this section we solve a simplified problem in which a single "predator" feeds upon an unevolving population of unit-mass "prey." The prey do not merge with one another but only with the predator, whose initial mass is equal to that of the prey. A slight additional simplification results from assuming that the prey population is infinite. We call this model "monotrophic" after the Greek *mono* (one) + *trophein* (to nourish). Our Monte-Carlo simulations of the full stochastic equation are well described by the monotrophic model in their later stages when (or if) the most massive particle exhibits runaway growth.

We work in time units τ such that the feeding rate of a unit-mass predator is unity, and we assume that the feeding rate increases as the $\nu^{\rm th}$ power of its mass. Let the predator start with mass equal one at time $\tau = 0$, and let $p(k,\tau)$ be the probability that it is in the $k^{\rm th}$ mass bin and correspondingly has mass $m_k = k$ after time τ. The probability that the predator will enter mass bin k during the brief time interval $(\tau, \tau + d\tau)$ is clearly $p(k-1,\tau) \times (k-1)^\nu \times d\tau$, and the probability that it will vacate bin k during the same interval is $p(k,\tau) \times k^\nu \times d\tau$. Hence the evolutionary equation and initial conditions for p are

$$\frac{dp}{d\tau}(k,\tau) = (k-1)^\nu p(k-1,\tau) - k^\nu p(k,\tau), \qquad \text{and} \quad p(k,0) = \delta_{k,1}. \tag{6}$$

One might suppose that $\dfrac{d}{d\tau}\displaystyle\sum_{k=1}^{\infty} p(k,\tau) = 0$, since the sum of the righthand sides (6) would appear to cancel, but after solving eqs. (6), one finds that

$$\phi(\tau) \stackrel{\rm def}{=} 1 - \sum_{k=1}^{\infty} p(k,\tau) \tag{7}$$

can be nonzero for $\tau > 0$. Clearly $\phi(\tau)$ is the probability that the predator is not to be found in any finite mass bin. So we interpret $\phi(\tau)$ as the probability that runaway growth has occurred. From eq. (6), $\phi(0) = 0$ and

$$\frac{d\phi}{d\tau}(\tau) = \lim_{k\to\infty} k^\nu p(k,\tau). \tag{8}$$

Hence, the runaway cannot occur until the mass probability function develops a power-law tail $p(k,\tau) \propto k^{-\nu}$. But $\sum_{k=1}^{\infty} p(k,\tau)$ must be finite (in fact ≤ 1), and the power-law tail has a convergent sum only if $\nu > 1$. So we conclude that runaway occurs in the monotrophic model only if $\nu > 1$.

To solve for $\phi(\tau)$, we take the Laplace transform $\tau \to z$ of eq. (6),

$$z\tilde{p}(k,z) \ - \delta_{k,1} = (k-1)^{\nu}\tilde{p}(k-1,z) - k^{\nu}\tilde{p}(k,z).$$

This is easily solved:

$$k^{\nu}\tilde{p}(k,z) = \prod_{\ell=1}^{k}\left(1+\frac{z}{\ell^{\nu}}\right)^{-1} \qquad (k \geq 1). \tag{9}$$

In view of eq. (8), the Laplace transform of ϕ is

$$\tilde{\phi}_{\nu}(z) = \frac{1}{z}\lim_{k\to\infty}\prod_{\ell=1}^{k}\left(1+\frac{z}{\ell^{\nu}}\right)^{-1}. \tag{10}$$

A subscript has been placed on $\tilde{\phi}_{\nu}(z)$ to acknowledge its dependence on ν. Standard convergence tests show that the limit of the product vanishes if $\nu \leq 1$ except at the poles $z = -1^{\nu}, -2^{\nu}, -3^{\nu}, \ldots$, so that $\phi_{\nu\leq 1}(\tau) = 0$ also vanishes. Once again, therefore, we see that runaway does not occur for $\nu \leq 1$. On the other hand, if $\nu > 1$ then the product has a finite nonzero limit.

Exact results are possible for $\nu = 2$. The product (10) has the closed form

$$\tilde{\phi}_2(z) = \frac{\pi}{\sqrt{z}\sinh(\pi\sqrt{z})}. \tag{11}$$

The only singularities of this function at finite z are simple poles on the negative real axis where $\sqrt{-z}$ is a positive integer. Evaluating the inverse Laplace transform by residues yields an infinite series that converges rapidly at large τ:[1]

$$\phi_2(\tau) = 1 + 2\sum_{k=1}^{\infty}(-1)^k e^{-k^2\tau} \tag{12}$$

Writing

$$\begin{aligned} \phi_2(\tau) &= \int_{-\infty}^{\infty}\Delta(x)\, e^{-\tau x^2}\, dx, \\ \text{where} \quad \Delta(x) &\stackrel{\text{def}}{=} \sum_{k=-\infty}^{\infty}(-1)^k\delta(x-k) = 2\sum_{n=0}^{\infty}\cos\left[(2n+1)\pi x\right], \end{aligned}$$

[1] $\phi_2(\tau)$ can also be expressed in a parametric closed form involving elliptic integrals.

and integrating the Fourier series term by term yields a series that converges rapidly at small times:

$$\phi_2(\tau) = 2\sqrt{\frac{\pi}{\tau}} \sum_{n=0}^{\infty} \exp\left[-\frac{\pi^2(2n+1)^2}{4\tau}\right]. \tag{13}$$

Eq. (13) shows that runaway is exponentially unlikely for $\tau \ll 1$, while eq. (12) shows that it is virtually certain for $\tau \gg 1$. The probability reaches 50% at $\tau \approx 1.37$.

Similar statements hold for general values of $\nu > 1$ (cf. the Appendix):

$$\phi_\nu(\tau) \approx \begin{cases} (2\pi)^{(\nu-1)/2}\sqrt{\nu/(\nu-1)\tau}\,\exp\left\{-(\nu-1)\left[\nu\sin(\pi/\nu)/\pi\right]^{-\nu/(\nu-1)}\,\tau^{-1/(\nu-1)}\right\} & \text{if } \tau \ll 1, \\ 1 \;-\; \left[\prod_{k=2}^{\infty}(1-k^{-\nu})\right]^{-1}\,\exp(-\tau) & \text{if } \tau \gg 1. \end{cases} \tag{14}$$

These expressions agree with the leading terms of the series (12) and (13) when $\nu = 2$. Scrutiny of the first exponential in eq. (14) reveals that as ν approaches unity from above, the time at which the runaway probability first becomes appreciably different from zero is $\approx (\nu-1)^{-1}$.

In the original model of §1, all particles can be predator or prey. For $\tau \ll 1$, the results of this section suggest that the probability that any given particle has achieved large mass is $\approx \phi(\tau)$. We presume these probabilities to be approximately independent if N is sufficiently large, because two randomly selected particles could both grow to a mass $\gg 1$ before competing for the same prey. Thus the *total* probability of runaway at a time $\tau << 1$ is $\approx N\phi(\tau)$. Given the estimate (14) for $\phi(\tau)$, the total runaway probability approaches unity at a time scaling as

$$\tau_{\rm runaway} \propto (\log N)^{\gamma(\nu)} \tag{15}$$

with $\gamma(\nu) = 1 - \nu < 0$, but only if $\nu > 1$. To test this conjecture, we undertook the Monte Carlo simulations described below.

3. Numerical Technique and Tests

Direct numerical solutions of the stochastic coagulation equation (3) are difficult to obtain for large N, so we have used Monte Carlo simulations. Great savings in memory and processor time can be achieved by keeping track of the occupied bins only. Therefore, we adopt an indexing scheme different from that of §1: at each time step, $n_i \neq 0$ will represent the occupation number of the $i^{\rm th}$ *nonempty* bin, with mass per particle m_i, and $1 \leq i \leq I$. For expository convenience, the bins are sorted by mass ($m_i < m_j$ if $i < j$), although this is

not essential to the algorithm. The total mass is

$$\sum_{i=1}^{I} n_i\, m_i = N. \tag{16}$$

The storage required by our scheme is $O(I)$. Because $m_i \geq i$ and $n_i \geq 1$, the summation (16) is $\geq I(I+1)/2$. Hence the number of occupied bins $I < (2N)^{1/2}$. In our simulations, the maximum I encountered is almost always much smaller than this upper bound.

The coagulation kernel is now written as $K(m_i, m_j)$ rather than $K(i,j)$ to emphasize that the coalescence rate depends upon the particle masses rather than the arbitrary bin indices. The total coalescence rate of bins $i, j \geq i$ is

$$R_{i,j} \stackrel{\text{def}}{=} K(m_i, m_j) \times \begin{cases} n_i n_j & i < j \\ n_i(n_i - 1)/2 & i = j \end{cases}. \tag{17}$$

It is useful to imagine these rates arranged as an $I \times I$ upper-triangular matrix, and to introduce the partial sums

$$S_{i,j} \stackrel{\text{def}}{=} \sum_{k=1}^{i-1} \sum_{\ell=k}^{I} R_{k,\ell} + \sum_{\ell=i}^{j} R_{i,\ell}, \tag{18}$$

i.e. $S_{i,j}$ is the sum of the first $i-1$ rows plus the first j columns of row i, and the total coalescence rate $S \stackrel{\text{def}}{=} S_{I,I}$. We store in the computer memory the rates $S_{i,I}$, $i = 1, 2, ...I$. Each merging alters the occupation numbers of at most three bins, so these rates can be updated in $O(I)$ operations. Indirect indexing minimizes the work of inserting or deleting rows and columns as the list of occupied bins changes.

Every simulation begins with monodisperse initial conditions,

$$n_1 = N, \quad m_1 = 1, \quad I = 1, \tag{19}$$

and ends after $N-1$ mergings with

$$n_1 = 1, \quad m_1 = N, \quad I = 1. \tag{20}$$

Merging occurs at random but increasing times $t_1 < t_2 \ldots \leq t_{N-1}$ chosen as follows: If S is the total coalescence rate computed after the s^{th} merging, the probability that no further merging occurs before $t > t_s$ is

$$\mathcal{P} = \exp\left[-S \cdot (t - t_s)\right].$$

Therefore, we chose a random number $X \sim U(0,1]$ (*i.e.*, X is uniformly distributed between 0 and 1) and take

$$t_{s+1} = t_s \; - S^{-1} \ln X.$$

Thus merging occurs at t_{s+1}, and the next task is to decide which bins are involved. Choosing a second random number $Y \sim U(0,1]$, we find i, j $(j \geq i)$ such that

$$S_{i,j-1} \ < \ Y \cdot S \ \leq \ S_{i,j}. \tag{21}$$

Since $S_{i,j} - S_{i,j-1} = R_{i,j}$ [eq. (18)], bins i, j are selected with the correct probability $R_{i,j}/S$, all rates being evaluated just before the $s+1^{\rm st}$ merging.

With this scheme, there are $N-1$ steps per simulation and $O(I)$ operations per step, so the number of operations per simulation is at most $O(N^{3/2})$. In practice, $I \ll N^{1/2}$ so that the computer time is almost linearly proportional to N. We average many simulations to obtain the statistics of quantities of interest.

We have tested our code against the exact solutions of Tanaka and Kiyoshi (1993) for the cases $K(m_i, m_j) = 1$ and $K(m_i, m_j) = m_i + m_j$. We compare at $N = 10$ and find excellent agreement (Fig. 1). Not surprisingly, even though runaway does not occur, the statistical model is a poor approximation at such small N.

4. SIMULATION RESULTS

We discuss simulations for two classes of coalescence rates, $K(m_i, m_j) = (m_i \times m_j)^\nu$ (*multiplicative* kernel) and $K(m_i, m_j) = (m_i + m_j)^\nu$, $\nu > 1$ (*additive* kernel).

Figure 2 shows the evolution of various averaged diagnostics for the representative case $\nu = 2$, $N = 10^7$ and for both additive and multiplicative kernels. Instead of elapsed time, we use the logarithm of the number of mergings, $N_{\rm merg}$, as the independent variable. Fig. 2(a) shows the (average) relationship between these coordinates. Note that we have reintroduced τ [cf. eq. (5)], which is time normalized to the collision time per particle in the initial state (19). We see that there are two evolutionary phases. In the first phase, the total coalescence rate is dominated by mergings among unit-mass particles [Fig. 2(d)]. The mass spectrum, *i.e.* the distribution of average occupation number $\overline{n}$ with particle mass m, is continuous, as shown by the near-equality of the largest and second-largest mass [Fig. 2(b)], and extends to steadily higher m [Figs. 2(e,c)]. The total coalescence rate is approximately equal to its initial value $N/2t_{\rm coll}$. This is the *statistical growth phase*.

The *runaway growth phase* could be considered to begin when there is a significant mass gap between the highest and second-highest occupied bin [Fig. 2(b)]. We find it more convenient to declare runaway when the rate of mergings involving the highest occupied bin is 50% of the total coalescence rate [Fig. 2(d)]. At this point m_I, the mass per particle of the highest-mass bin, is $\approx N^{1/\nu}$. The runaway phase accounts for a negligible fraction of the

total time (t or τ) but a majority of the total mergings [Fig. 2(a)].

For other coalescence exponents $\nu > 1$, the qualitative features of the evolution are similar to those displayed in Fig. 2 at sufficiently large N. As ν approaches unity, larger N is required to obtain similar behavior, and runaway begins later—*i.e.*, at larger $N_{\rm merge}/N$.

At a given N and ν, runaway occurs later for additive than for multiplicative kernels and involves more particles of intermediate mass. The latter is explained by the fact that the collision rate between particles of very different mass is almost independent of the lighter mass with the additive kernel. Once the runaway phase of the multiplicative case is well established, most of the particles are of unit mass, and the evolution is similar to the monotrophic model [Fig. 2(e,f)].

Figure (3) shows that the runaway time slowly decreases with increasing N, even after scaling by the single-particle collision time (5). At sufficiently large N, it appears that $\tau_{\rm runaway}$ decreases as a power of $\log N$ and that the slope is steeper for larger ν, in qualitative agreement with the conjecture (15). The first panel of Fig. (4) shows rough quantitative agreement with the conjecture in the slope of $\gamma(\nu)$ against ν for multiplicative kernels. There appears to be an offset in the vertical intercept, but one knows from the exact results of Lushnikov (1977) that $\tau_{\rm runaway}$ is independent of N as $N \to \infty$ at $\nu = 1$, so the solid and dashed lines should intersect at $\gamma(1) = 0$. Unfortunately, it is extremely difficult to measure γ near $\nu = 1$ from our simulations. The second panel of Fig. (4) shows that for additive kernels, the empirical slope of $\gamma(\nu)$ is close to one half of the prediction (15).

5. DISCUSSION

Our Monte Carlo simulations indicate that runaway is instantaneous in the limit $N \to \infty$ if the coalescence kernel is superlinear, in agreement with previous authors (Jeon 1999; Spouge 1985). But the simulations, as well as the heuristic model of §2, suggest a more quantitative new result: namely, that the limit $\tau_{\rm runaway} \to 0$ is approached only logarithmically in N for power-law kernels.

We consider briefly two astrophysical applications: coalescence of planetesimals into planets in a protostellar disk, and black hole formation through stellar mergers in galactic nuclei. In both cases, the two-body collision rate per unit volume is $\nu_i \nu_j \langle \sigma v \rangle_{ij}$, where ν_i is the number of particles of mass m_i per unit volume, and the rate coefficient is approximately (Lee 2000)

$$\langle \sigma v \rangle_{ij} = \pi (R_i + R_j)^2 \left[v_{ij} + \frac{2G(m_i + m_j)}{(R_i + R_j)} \frac{1}{v_{ij}} \right]. \tag{22}$$

Here R_i is the radius corresponding to mass m_i, and v_{ij} is the root-mean-square relative velocity of the particles. The prospects for runaway are usually more favorable when the second (*gravitational focusing*) term in the square brackets above is dominant. Henceforth, we neglect the first term. A power-law mass-radius relation

$$R \propto m^{\alpha} \tag{23}$$

describes planetesimals if $\alpha \approx 1/3$, and stars if $\alpha \approx 1$. For a maxwellian velocity distribution with equipartition of kinetic energies among mass groups,

$$v_{ij} = v_1 \left(\frac{i+j}{ij} \right)^{1/2},$$

where v_1 is the velocity dispersion of particles of mass m_1 and $m_i = i \times m_1$. Then

$$\langle \sigma v \rangle_{ij} \approx \frac{2\pi G m_1 R_1}{v_1} \, (i^{\alpha} + j^{\alpha}) \, (i+j)^{1/2} (ij)^{1/2} \tag{24}$$

Since this is proportional to $j^{\alpha+1}$ for $j \gg i$, runaway is possible if $\alpha > 0$.

Mass stratification somewhat intensifies the tendency towards runaway. A large-scale gravitational potential will concentrate the heavier particles into a smaller volume than the lighter ones. Thus in a disk of planetesimals with orbital angular velocity Ω, the distribution of mass group i with height z above the midplane is

$$\nu_i(z) \approx \nu_i(0) \exp\left(-z^2/2H_i^2\right), \qquad H_i \equiv v_i/\Omega \propto i^{-1/2}.$$

Hence upon integrating with respect to z,

$$\int_{-\infty}^{\infty} \nu_i(z) \nu_j(z) \, dz = \left(2\pi H_1^2\right)^{-1/2} \, \hat{n}_i \hat{n}_j \, \left(\frac{ij}{i+j} \right)^{1/2}. \tag{25}$$

Here $\hat{n}_i$ is the number of particles of mass m_i per unit area. The mass-dependent factor in this expression multiplies the rate coefficient (24) to yield an effective collision kernel ($\alpha \approx 1/3$)

$$K(i,j) = K(1,1) \, \times \, ij \, (i^{1/3} + j^{1/3})/2, \tag{26}$$

which has the same $j^{4/3}$ scaling for $j \gg i$ as the rate coefficient (24) but a stronger dependence on the mass of the lighter particle: i versus $i^{1/2}$. This is likely to cause more rapid consumption of intermediate-mass objects, so we expect evolution as if for a multiplicative kernel [$K(i,j) \propto (ij)^{4/3}$] rather than an additive one [$K(i,j) \propto (i+j)^{4/3}$].

The situation in galactic nuclei is more complicated if the heavier stars concentrate into a selfgravitating population. Setting aside this possibility (which would make runaway still more rapid) and assuming a harmonic mean potential, we get in place of eq. (25)

$$\int_0^\infty \nu_i(r)\nu_j(r)\,4\pi r^2 dr = \frac{n_i n_j}{2(2\pi)^{5/2}H_1^3}\left(\frac{ij}{i+j}\right)^{3/2},$$

since the geometry is spherical rather than planar. Here n_i is the total number of particles of type i. So in this case, with $\alpha = 1$,

$$K(i,j) = K(1,1)\,\times\,(ij)^2. \tag{27}$$

This is precisely our multiplicative $\nu = 2$ kernel.

As many as $\sim 10^{11}$ asteroid-sized planetesimals are required to make up the mass of a terrestrial planet. The smallest coalescence exponent for which our simulations give reliable averages for $\tau_{\rm runaway}$ is $\nu = 3/2$, and the largest N we have used is 10^9. Nevertheless, by extrapolating the curves in Fig. (3), we estimate $t_{\rm runaway} \approx 0.4\,t_{\rm coll}$ at $N = 10^{11}$, versus $t_{\rm runaway} \approx 2\,t_{\rm coll}$ at $N = 10^2$. The dependence on $\log N$ is somewhat stronger than one would expect from the asymptotic scaling (15) because of the curvature in Fig. (3).

Black holes associated with quasars in the nuclei of galaxies are thought to have masses of order $10^{8-9}\,M_\odot$. The prevailing wisdom is that the black hole forms by accretion from a gas disk, but formation by stellar coalescence has long been a popular alternative model (Rees 1984, and references therein). Referring again to Fig. (3), but now for $\nu = 2$, we find $t_{\rm runaway} \approx .09\,t_{\rm coll}$ at $N = 10^9$ versus $t_{\rm runaway} \approx .35\,t_{\rm coll}$ at $N = 10^2$, roughly in agreement with the predicted asymptotic scaling $(\log N)^{1-\nu}$.

REFERENCES

Bender, C. M., and Orszag, S. A. 1978. *Advanced Mathematical Methods for Scientists and Engineers.* New York, McGraw-Hill.

Domilovskii, E. R., Lushikov, A. A., and Piskunov, V. N. 1978. Monte Carlo Simulation of Coagulation Processes *Doklady Physical Chemistry* **240**, 108-110.

Flory, P. J. 1953. *Principles of Polymer Chemistry.* Cornell Univ. Press, Ithaca, New York.

Jeon, I. 1999. Spouge's Conjecture on Complete and Instantaneous Gelation. *Journal of Statistical Physics* **96**, 1049-1070.

Lee, H. M. 1987. Dynamical Effects of Successive Mergers on the Evolution of Spherical Stellar Systems. *Astrophys. J.* **319**, 801.

Lee, M. H. 2000. On the Validity of the Coagulation Equation and the Nature of Runaway Growth. *Icarus* **143**, 74-86.

Lushnikov, A. A. 1977. Coagulation in Finite Systems. *Journal of Colloid and Interface Science* **65**, 276-285.

Quinlan, G. D., and Shapiro, S. L. 1990. Dynamical Evolution of Dense Star Clusters in Galactic Nuclei. *Astrophys. J.* **356**, 483-500

Rees, M. J. 1984. *Ann. Rev. Astr. Astrophys.* **22**, 471.

Safronov, V. S. 1969. *Evolution of the Protoplanetary Cloud and Formation of the Earth and the Planets*. Nauka, Moscow. Transl. Israel Program for Scientific Translations, **v. 206**, NASA Technical Translations NASA-TT F-677 (1972).

Smoluchowski, M. von. 1916. *Zeitschrift für Physik* **17**, 557; 585

Spouge, J. L. 1985. Monte Carlo Results for Random Coagulation. *Journal of Colloid and Interface Science* **107**, 38-43

Tanaka, H., and Kiyoshi, N. 1993. Stochastic Coagulation Equation and Validity of the Statistical Coagulation Equation. *J. Geomag. Geoelectr.* **45**, 361-381.

Trubnikov, B. A. 1971. Solution of the coagulation equations in the case of a bilinear coefficient of adhesion of particles. *Sov. Phys. Dokl.* **16**, 124-126.

A. Asymptotics of the monotrophic runaway probability

To derive eqs. (14), one must approximate the inverse Laplace transform

$$\phi_\nu(\tau) = \frac{1}{2\pi i} \int_{C-i\infty}^{C+i\infty} \tilde{\phi}_\nu(z) e^{z\tau}\, d\tau, \tag{A1}$$

with $\tilde{\phi}_\nu(z)$ represented by the infinite product (10). The real constant C must be positive but is otherwise arbitrary, since the integrand is analytic for Re(z) > 0. Clearly, $\tilde{\phi}_\nu(z)$ decreases

rapidly as Re(z) > 0 increases, while $e^{z\tau}$ has the opposite trend. A good choice for C is the point C_0 along the real axis where the product of these two factors in the integrand (A1) is smallest. By analyticity, this is actually a saddle point with respect to complex z, so the integrand will further decrease along the integration contour with increasing $|\mathrm{Im}(z)|$. For $\tau \ll 1$, $C_0 \gg 1$, because the exponential varies only slowly; whereas for $\tau \gg 1$, C_0 lies close to the pole of $\tilde{\phi}_\nu(z)$ at $z = 0$.

Thus for small τ, we are concerned with Re(z) $\gg 1$. We rewrite eq. (10) as

$$\ln\left[z\tilde{\phi}(z)\right] = -\sum_{k=1}^{\infty} \ln\left(1+\frac{z}{k^\nu}\right) \;\; = -\lim_{n\to\infty}\left[\sum_{k=1}^{n} \ln\left(1+\frac{k^\nu}{z}\right) \;+\; \ln\frac{z^n}{(n!)^\nu}\right] \tag{A2}$$

The latter sum is dominated by its upper limit and can be approximated by the leading terms of the Euler-Maclaurin formula (Bender and Orszag 1978):

$$\begin{aligned}\sum_{k=1}^{n} \ln\left(1+\frac{k^\nu}{z}\right) \;&\approx\; \int_0^n \ln\left(1+\frac{x^\nu}{z}\right) dx \;+\; \frac{1}{2}\ln\left(1+\frac{n^\nu}{z}\right) \\ &=\; \left(n+\frac{1}{2}\right)\ln\left(1+\frac{n^\nu}{z}\right) - n\nu \;+\nu z\int_0^n \frac{dx}{z+x^\nu},\end{aligned}$$

where integration by parts has been used. As $n \to \infty$, the latter integral becomes

$$\nu z\int_0^\infty \frac{dx}{z+x^\nu} = \nu z^{1/\nu}\,\Gamma\left(\frac{1}{\nu}\right)\Gamma\left(1-\frac{1}{\nu}\right) = z^{1/\nu}\,\frac{\pi}{\sin(\pi/\nu)}.$$

After this is substituted into eq. (A2) and Stirling's approximation is used for $n!$, the terms growing with n cancel, and upon taking $n \to \infty$ one has

$$\ln\tilde{\phi}(z) \approx -\frac{\pi z^{1/\nu}}{\sin(\pi/\nu)} - \frac{1}{2}\ln z + \frac{\nu}{2}\ln(2\pi) \;+O(z^{-1}). \tag{A3}$$

Using this, we estimate

$$C_0 = \left[\frac{\pi}{\tau\nu\sin(\pi/\nu)}\right]^{\nu/(\nu-1)}$$

and then perform a straightforward steepest-descent contour integration, *i.e.* we expand $\ln\tilde{\phi}(z) + z\tau$ as a Taylor series to second order in z about $z = C_0$ and use the resulting Gaussian to approximate the integrand (A1). This gives the upper line in eq. (14).

For $\tau \gg 1$, we evaluate (A1) from the residues of the poles at $z = 0$ and $z = -1$; the remaining residues are strongly suppressed by the exponential factor. This yields the lower line in eq. (14).

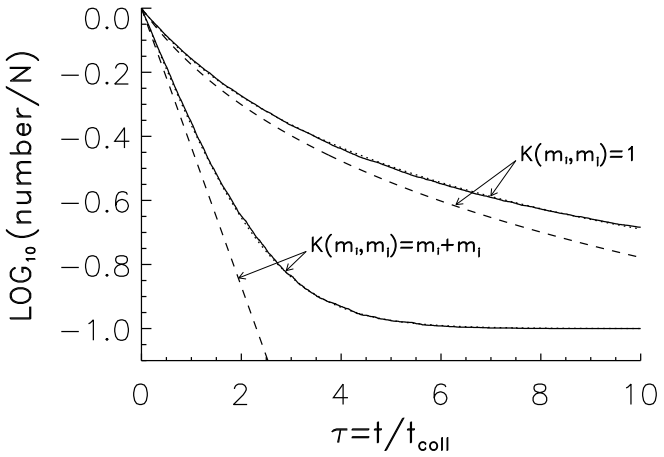

Fig. 1.— The number of particles, averaged over 1000 simulation runs and normalized to the initial number of particles ($N = 10$), versus our dimensional time is shown by the two solid lines. The analytical results for the stochastic and statistical coagulation equations are shown by the two dotted lines (which almost coincide with the corresponding solid lines) and two dashed lines respectively.

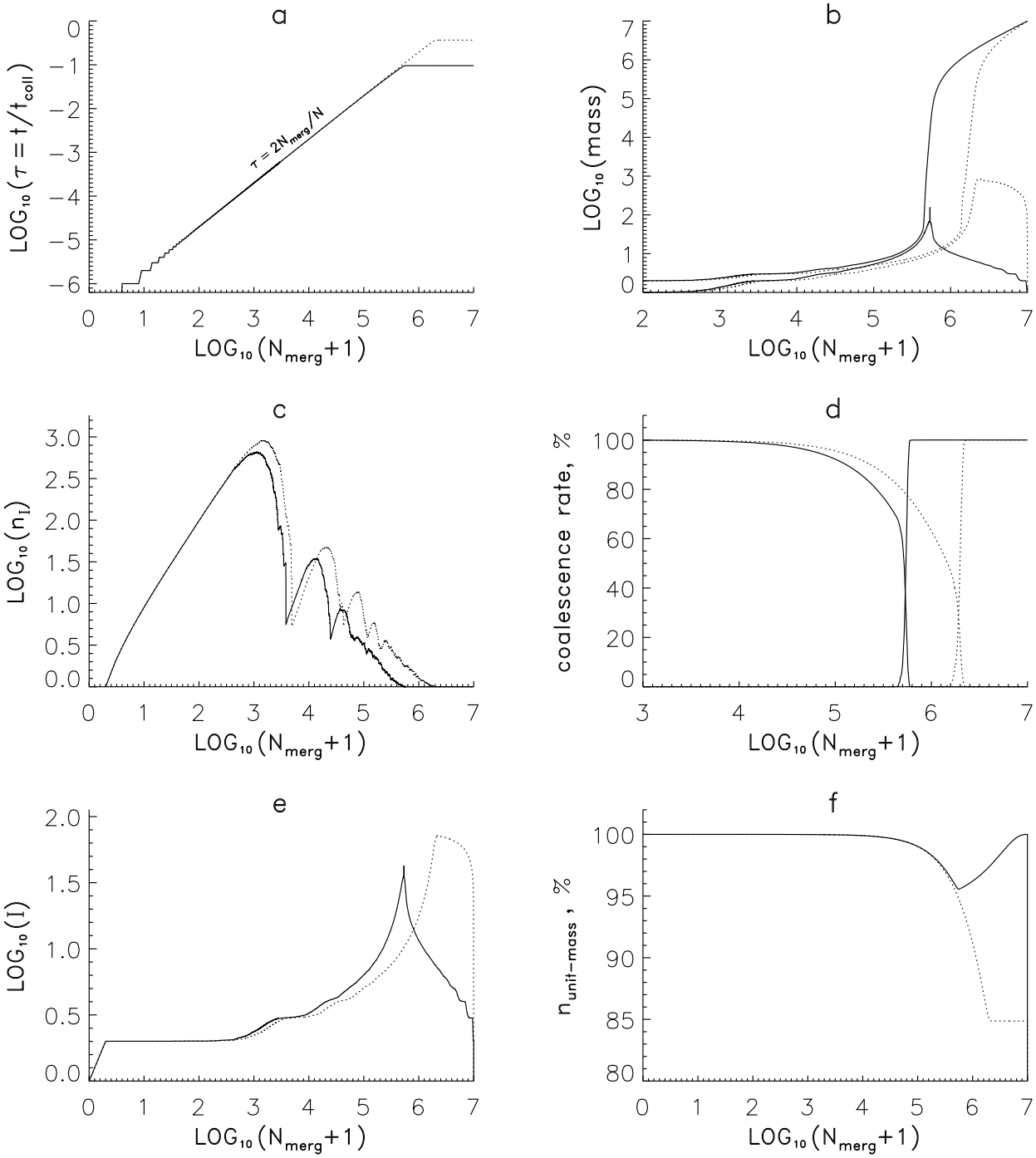

Fig. 2.— Average evolution for 300 simulations with $N = 10^7$. Solid lines: $K(m_i, m_j) = (m_i \times m_j)^2$; dotted lines: $K(m_i, m_j) = (m_i + m_j)^2$. (a): time versus number of mergings, $N_{\rm merg}$; (b): the mass per particle of the highest (monotonic curves) and the second highest bins, *i.e.* m_I and m_{I-1}; (c): the number of particles in the highest bin; (d): fraction of the total coalescence rate that involves one particle taken from the highest bin (monotonically increasing), and by mergings between unit-mass particles (decreasing); (e): number of occupied mass bins, I; (f): number of unit-mass particles as a fraction of the total remaining, *i.e.* $\delta_{1,m_1}\, n_1/(N - N_{\rm merge})$.

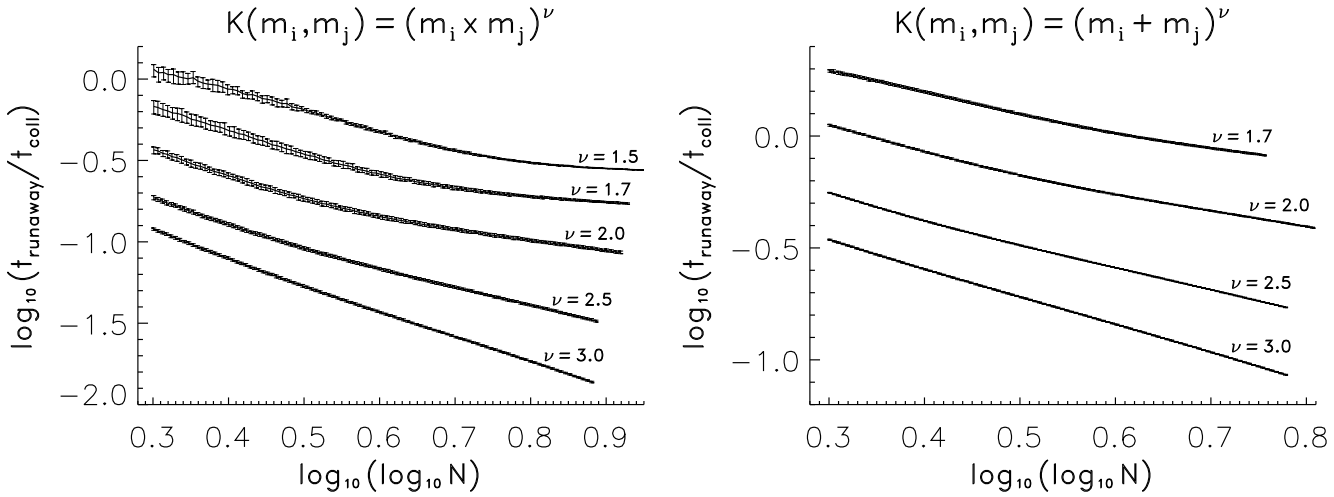

Fig. 3.— Average normalized time at which runaway begins versus initial particle number N for different coalescence exponents ν. Error bars enclose 50% of the simulations [$30 - 10^5$ simulations at each (N, ν)].

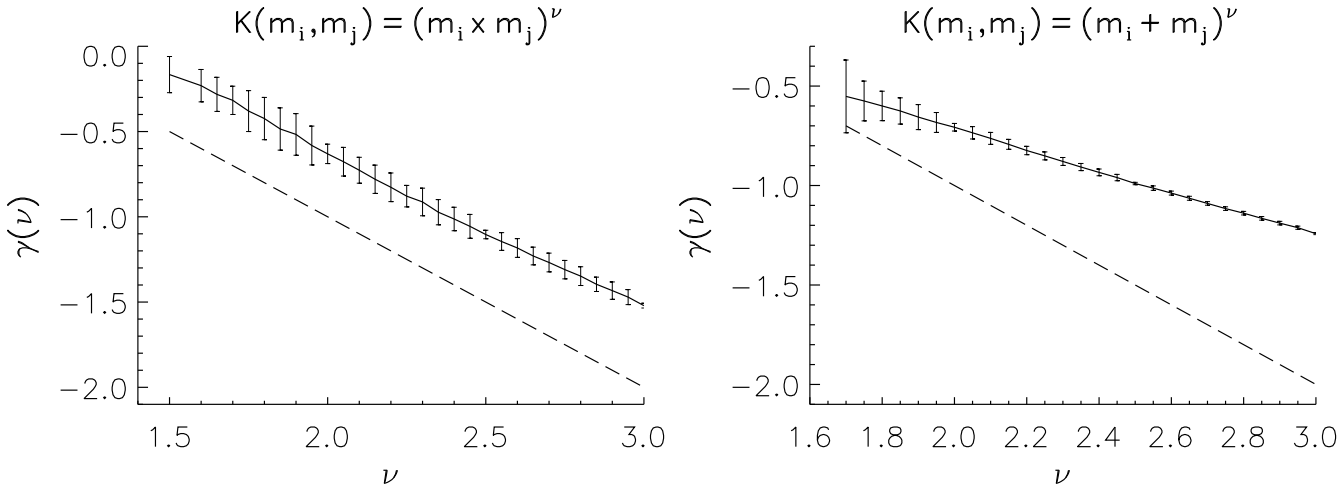

Fig. 4.— Exponent γ for the relation $\tau_{\rm runaway} \propto (\log N)^\gamma$ between runaway time and particle number, versus coalescence exponent ν. Solid lines: best fit based on asymptotic slope seen in Fig. 3 at large N (the slope and error bars are obtained by the least-squares linear regression). Dashed lines: prediction $\gamma = 1 - \nu$ of monotrophic model [eq. (15)].